Original Article
Heat shock protein 70-2 (HSP70-2) a novel cancer testis antigen that promotes growth of ovarian cancer

Namita Gupta[1], Nirmala Jagadish[1], Avadhesha Surolia[2], Anil Suri[1]

[1]Cancer Microarray, Genes and Proteins Laboratory, National Institute of Immunology, Aruna Asaf Ali Marg, New Delhi-110 067, India; [2]Molecular Biophysics Unit, Indian Institute of Science, Bangalore 560012, India

Abstract: Heat shock protein 70-2 (HSP70-2) is known to be involved in tumor progression. However, its molecular role and mechanism in epithelial ovarian cancer (EOC) remains unknown. In the present investigation, we examined the role of HSP70-2 in cell cycle, apoptosis and epithelial mesenchymal transition pathways in EOC cells in *in vitro* and *in-vivo* xenograft mouse model. To investigate the role of HSP70-2 in ovarian cancer, plasmid driven short hairpin RNA approach was used to examine HSP70-2 gene and protein expression in ovarian cancer cell line A-10 (origin: serous papillary cystadenocarcinoma), Caov-3 (origin: adenocarcinoma) and SKOV3 (origin: adenocarcinoma; derived from metastatic site: ascites) by RT-PCR, quantitative-PCR, immunohistochemistry and Western blotting. Light microscopy, scanning electron microscopy, viability tests, and flow cytometry were used to study the cellular proliferation, onset of senescence, colony forming ability and morphological features of cancer cells. Cell migration and invasion ability was evaluated by wound healing and Boyden chamber assays. Further, we studied the effect of HSP70-2 protein ablation on human ovarian xenograft mice model. At molecular level, various molecules involved in apoptosis, cell cycle and epithelial-mesenchymal-transition were also examined both in *in-vitro* and *in-vivo* xenograft mouse model. The knockdown of HSP70-2 expression by gene silencing resulted in the onset of apoptosis, senescence, reduced cellular growth and colony forming ability of EOC cells. Interestingly, the migration, invasion and wound healing abilities of cells were also significantly inhibited. In addition, the ablation of HSP70-2 resulted in the upregulation of cytochrome-C, caspase 3, caspase 7, caspase 9, APAF1, BAX, BIM, BAK, BAD, BID, PUMA, NOXA, p16, p21, Rb, E-cadherin, cytokeratin 18, EMA in these cells as well as in the xenograft tumor specimens. However, there was downregulation of PARP1, BCL-2, Bcl-x$_L$, MCL-1, Survivin, XIAP, cIAP2, CDK1, CDK2, CDK4, CDK6, cyclin D1, cyclin E, cyclin A2, cyclin B1, p-Rb, N-cadherin, SNAIL, SLUG, VIMENTIN, SMA, MMP2, MMP3, MMP9 and TWIST in these samples. Furthermore, the xenograft studies showed significant reduction in the tumor growth. Our results suggest that HSP70-2 can promote cellular growth and invasion of EOC cells and therefore may be a potential therapeutic target in EOC.

Keywords: HSP70-2, gene silencing, migration, invasion, tumor regression, ovarian cancer

Introduction

Ovarian cancer is the most lethal gynecological cancer worldwide [1]. Majority of the ovarian cancers are diagnosed at advanced stage because of which the treatment options are limited [2]. Among ovarian cancer, epithelial ovarian cancer (EOC) of serous histotype is the most prevalent and aggressive subtype [3]. Recently, cancer testis (CT) antigens have been the main focus of research for exploring novel therapeutics for cancer treatment [4]. CT antigens are unique class of tumor associated antigens which are highly immunogenic and are abundantly expressed in various malignancies but not in somatic tissues except testis [5] and hence may be a potential target for novel therapeutic approach. In this context, a novel CT antigen, heat shock protein 70-2 (HSP70-2) a member of HSP70 family protein [6], has been demonstrated to be expressed in various malignancies [6-11] and is being investigated as a target for development of novel therapeutics. HSP70-2 has been proposed to be involved in the formation of an active complex of CDC2/Cyclin B during metaphase of the first meiotic division in germ cells during spermatogenesis [12], suggesting that it is a chaperone

necessary for the progression of meiosis in the germ cells [13]. Moreover, in *HSP70-2* gene knock-out [Hsp70-2(-/-)] mice, it was demonstrated that primary spermatocytes failed to complete meiosis, indicating a link between HSP70-2 and CDC2 kinase activity during this phase of spermatogenesis [12].

Recently, our laboratory has shown that HSP-70-2 is involved in cellular proliferation, early spread and progression of bladder cancer [7], cervical cancer [8], breast cancer [9] and colorectal [10]. However, the role of HSP70-2 in various molecular pathways contributing towards cellular proliferation, migration and invasion ability in EOC cells remains unclear. Therefore, there is a need to understand the role of HSP70-2 in EOC in order to delineate the underlying mechanisms for developing a new therapeutic target for better cancer management.

The molecular pathology of EOC is heterogeneous and involves alterations in various pathways which contribute to multistep and multi-factorial carcinogenesis. Defects in cell signaling and epithelial-mesenchymal transition (EMT) pathways play a vital role in cancer cell growth, survival, invasion and metastasis. Here, we have investigated the effect of knockdown of HSP70-2 on various properties of ovarian cancer cells using in *in-vitro* and *in-vivo* human ovarian xenograft mouse model and studied its role in various pathways contributing towards ovarian carcinogenesis. Our study has put forth evidence that HSP70-2 promotes cellular growth and multistep motility process since its ablation result in cell cycle arrest, onset of senescence state, apoptosis and inhibits cellular motility. The resulting changes were confirmed both at morphological and at molecular levels. *In-vivo* studies carried out in immuno-compromised mice model corroborated our cell culture findings. Thus, HSP70-2 may be a potential target for developing as a new treatment modality for ovarian cancer.

Material and methods

Cell lines and culture

Ovarian cancer cell line, A-10 (origin: serous papillary cystadenocarcinoma) is a kind gift from Dr. Kunle Odunsi (Roswell Park Cancer Institute, Buffalo, NY). Caov-3 (origin: ovary, adenocarcinoma) and SKOV3 (origin: ovary; adenocarcinoma; derived from metastatic site: ascites) were procured from American Type Culture Collection (ATCC, Manassas, USA). A-10 and Caov-3 cell were cultured in Dulbecco's Modified Eagle Media (DMEM) with 10% Fetal Bovine Sera (FBS) and SKOV3 in McCoy's 5A media with 15% FBS and maintained at 37°C with 5% CO_2 incubator. The cell lines were used within a month of procurement and mycoplasma contamination was checked by mycoplasma PCR detection kit (Applied Biological Materials Inc., Richmond, Canada).

HSP70-2 mRNA expression by reverse transcription-polymerase chain reaction (RT-PCR)

HSP70-2 mRNA expression was checked by RT-PCR in all three ovarian cancer cells as described earlier [14]. RT-PCR was carried using *HSP70-2* specific primers as mentioned in Supplementary Table 1. *β-actin* was used as a loading control. The PCR product was electrophoresed on 2% agarose gel and sub-cloned into TOPO vector to confirm the nucleotide sequence.

HSP70-2 protein expression validation by Western blotting, indirect immunofluorescence (IIF) and flow cytometry

In order to investigate the HSP70-2 protein expression in ovarian cancer, Western blotting was carried out as described earlier [14] using rabbit anti-HSP70-2 antibody as primary antibody and goat anti-rabbit IgG Horseradish Peroxidase [HRP, (Jackson Immuno-Research Laboratories, Inc., Baltimore, USA)] as secondary antibody. The flow cytometric analysis was performed as described earlier [14] by incubating fixed cells with rabbit anti-HSP70-2 antibody and subsequently with donkey anti-rabbit IgG FITC. IIF was carried out to investigate HSP70-2 localization in various organelles of cancer cells as described earlier [14]. The images were acquired using Carl Zeiss LSM 510 meta confocal microscope (Germany).

Plasmid-based shRNA gene silencing, quantitative-PCR and Western blotting

To study the various malignant properties of ovarian cancer cells, gene silencing approach was employed using plasmid driven small interfering RNA. Four HSP70-2 shRNA plasmids and

the negative control (NC) shRNA plasmid were procured from SureSilencing shRNA plasmids (SuperArray, Frederick, MD, USA) as detailed earlier [7]. Post 48 hours of transfections, total RNA was isolated from transfected cells using RNeasy mini kit (Qiagen, Germany). Quantitative-PCR (qPCR) was performed as described earlier [14] using HSP70-2 primers. *β-actin* was included as an internal control. Similarly, qPCR analysis was carried out for various molecules involved in apoptosis, cell cycle and EMT pathway using primers as listed in Supplementary Tables 1 and 2. In addition, Western blotting was carried out as described earlier [14] to check the HSP70-2 protein expression post transfection with four HSP70-2 shRNA targets as compared to NC shRNA transfected cells. Western blot analysis was also done similarly for various molecules involved in apoptosis, cell cycle and EMT using specific antibodies as mentioned in Supplementary Information. The two shRNA targets that showed maximum ablation of HSP70-2 gene and protein expression were selected for all subsequent experiments.

Cellular proliferation, cell viability and colony forming ability

Effect of ablation of HSP70-2 protein was assessed as described earlier [14]. Cellular growth of cells transfected with NC shRNA, HSP70-2 shRNA3 and shRNA4 was assessed as described earlier [14]. For checking cell viability, cells transfected with NC shRNA, HSP70-2 shRNA3 and shRNA4 were seeded in a 96-well plate. Subsequently MTT assay was performed as described earlier [14]. Further, colony forming ability was carried out as described earlier [14]. The experiments have been performed three independent times and in triplicates.

Scanning electron microscopy

Cells transfected with NC shRNA, HSP70-2 shRNA3 and shRNA4 were fixed and processed at different time intervals as described earlier [14]. The images were captured using electron microscope (EVO LSM10 Zeiss, Germany) at 20 kV using SmartSEM software. As controls, ovarian cancer cells were also treated with paclitaxel (2.5 µM) and DMSO (1.5%).

Annexin V staining

To study the effect of HSP70-2 shRNA3 and shRNA4 on apoptosis as compared to NC

shRNA, transfected cells were stained with annexin V using annexinV-PerCP-Cy5-5-A staining kit (Biovision, Milpitas, CA, USA) and assay carried out as described earlier [14]. The experiments have been performed three independent times and in triplicates.

TUNEL assay

TUNEL assay was carried out to assess the DNA damage in HSP70-2 shRNA3 and shRNA4 treated cells using Apo-BrdU-Red in-situ DNA fragmentation assay kit (Biovision, Milpitas, CA, USA) as described earlier [14]. The experiments have been performed three independent times and in triplicates.

M30 assay

M30 assay was carried out to determine apoptotic events in cells and to detect the epitope of cytokeratin 18 presented on the surface of cells after cleavage of caspases. The assay was carried out as described earlier [14]. The experiments have been performed three independent times and in triplicates.

Cell cycle analysis by Propidium Iodide (PI) staining using flow cytometry

Cells transfected with NC shRNA, HSP70-2 shRNA3 and shRNA4 were fixed in 70% ethanol and treated with PI (25 µg/ml) and RNA-ase (10 µg/ml) solution for 30 min. The acquisition-analysis was done using BD-FACS CALIBUR (BD Biosciences, California, USA). The experiments have been performed three independent times and in triplicates.

Cellular senescence assay

Cells were transfected with NC shRNA, HSP70-2 shRNA3 and shRNA4 and β-galactosidase activity was assessed using Senescence kit (Sigma-Aldrich, St. Louis, MO, USA) as described earlier [14]. The experiments have been performed three independent times and in triplicates.

Cell migration, invasion and wound healing assay

Cellular motility was analyzed by carrying out cell migration and invasion assay as described earlier [14]. In addition, wound healing assay was also performed. Cells transfected with NC shRNA, HSP70-2 shRNA3 and shRNA4 were
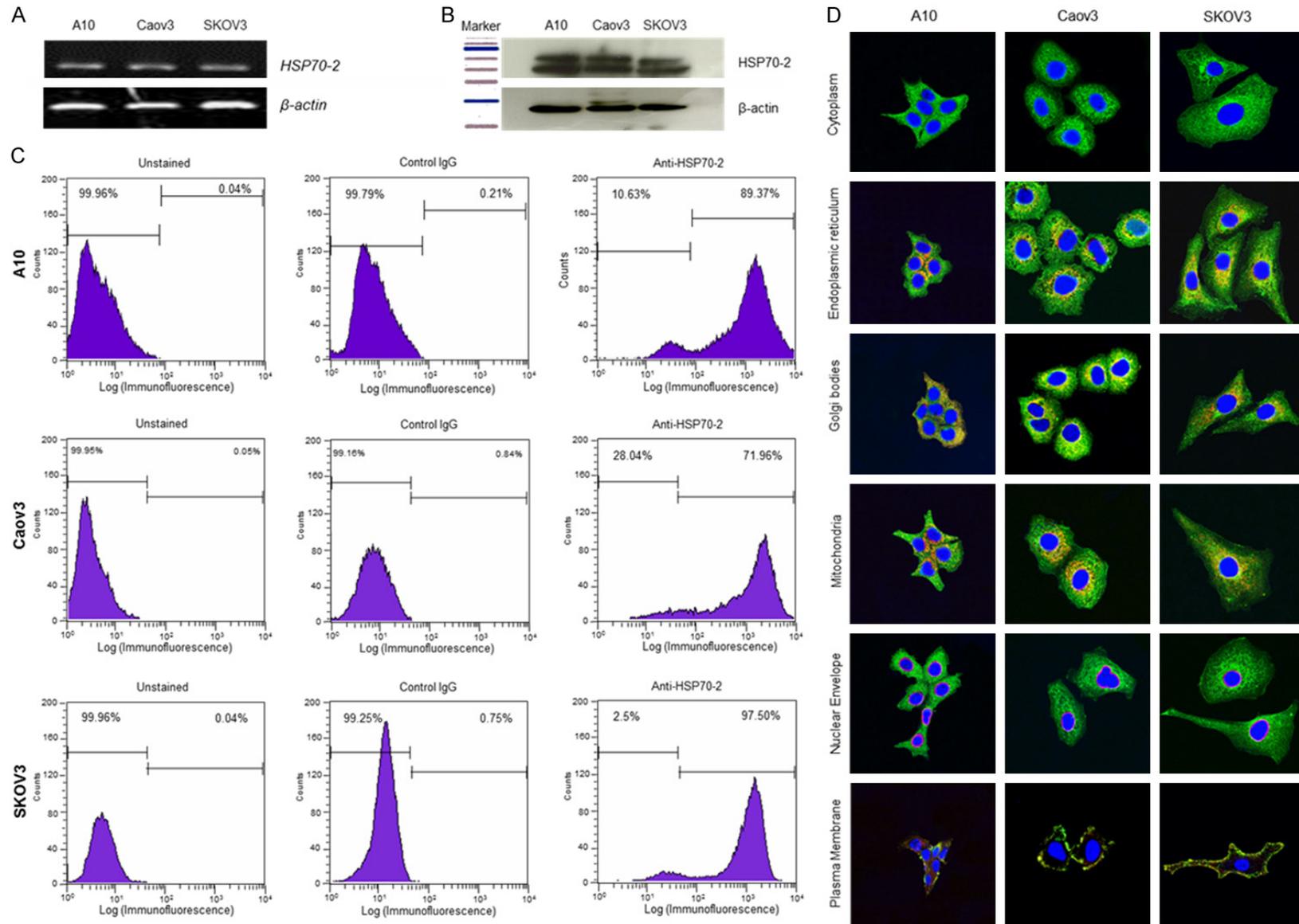
Figure 1. HSP70-2 gene and protein expression in ovarian cancer cell lines. A. RT-PCR analysis depicts HSP70-2 mRNA expression in A10, Caov3 and SKOV3 cells. B. Western blotting demonstrates the presence of 70 KDa HSP70-2 protein in ovarian cancer cells. β-actin was used as a loading control. C. Flow cytometric analyses show surface expression of HSP70-2 protein showing displacement in fluorescence intensity on x-axis, in ovarian cancer cells. Left panel shows unstained popula-

tion, middle panel shows population stained with control IgG antibody and right panel shows population stained with anti-HSP70-2 antibody. D. Indirect immunofluorescence images show cytoplasmic localization (green color) of HSP70-2 in ovarian cancer cells. Co-localization studies depicted HSP70-2 co-localization (orange-yellowish staining) in endoplasmic reticulum, Golgi bodies and mitochondria, however, no co-localization was observed in nuclear envelope. Original magnification ×630, objective ×63. The experiments were performed three independent times in triplicates.

seeded in a 35 mm culture dish and a scratch was made at 100% confluency. Photomicrographs were taken till 48 hour at every 12 hour interval. The experiments have been performed three independent times and in triplicates.

Effects of HSP70-2 shRNA on the growth of ovarian xenograft in immunocompromised mice

In-vivo studies were carried out to examine the effects of HSP70-2 ablation on the malignant properties of ovarian cancer. All investigations were conducted after obtaining ethical clearance from Institute animal ethical committee (IAEC). Human ovarian tumor xenograft using A-10 epithelial ovarian cancer cell line was established in immunocompromised SCID mice. When 50-100 mm^3 of tumor volume was achieved, the mice were divided into two groups of eight mice each; control and experimental. Subsequently, intra-tumor injections of the NC shRNA or shRNA3 (50 µg) were administered to the control or experimental group respectively. After 49 days, animals were euthanized, tumor excised and processed to study HSP70-2 expression. Total RNA was isolated and tumor lysates were prepared from the tumor specimens to study the quantification of gene expression by qPCR and protein validation by Western blotting of various molecules involved in apoptosis, EMT and cell cycle. In addition, immunohistochemistry (IHC) was carried out as described earlier [14] to check HSP70-2 protein expression, proliferating cell nuclear antigen (PCNA) and other molecules involved in different pathways.

Statistical analysis

The statistical analysis was done using SPSS 20.0 statistical software package (SPSS Inc., Chicago, USA) for all *in-vitro* and *in-vivo* assays to check the significance of *P* value using student's *t*-test (two-tailed). Survival curves were established using the Kaplan-Meier method. Data are expressed as mean ± standard error of the mean of three independent experiments

in triplicates in *in-vitro* assays. A *P*-value of less than 0.05 was considered statistically significant.

Results

HSP70-2 gene and protein expression in ovarian cancer cells

HSP70-2 gene and protein expression was examined in A10, Caov3, and SKOV3 ovarian cancer cell lines. RT-PCR analysis showed *HSP70-2* gene expression in all cell lines (**Figure 1A**). Further, Western blotting confirmed HSP70-2 protein expression in these cells (**Figure 1B**). Next we examined the expression of HSP70-2 on the cell surface of ovarian cancer cells by flow cytometry which revealed displacement of fluorescence intensity on x-axis, 89.37%, 71.96% and 97.5% of A10, Caov3, and SKOV3 cells, respectively when probed with anti-HSP70-2 antibody as compared to 0.04%, 0.05% and 0.04% unstained cells respectively (**Figure 1C**). Further, our co-localization studies revealed localization of HSP70-2 protein in endoplasmic reticulum, Golgi bodies, mitochondria and plasma membrane but not in the nuclear envelope (**Figure 1D**).

Ablation of HSP70-2 inhibits cellular proliferation, cell viability and colony forming ability

Gene silencing approach was employed using HSP70-2 shRNA to study the effect of HSP-70-2 ablation on cellular proliferation, cell viability and colony forming ability. Quantitative-PCR (qPCR, **Figure 2A**) and Western blotting (**Figure 2B**) analyses demonstrated that HSP70-2 shRNA3 and shRNA4 were able to knockdown HSP70-2 gene and protein most efficiently as compared to NC shRNA, shRNA1 and shRNA2. Hence, HSP70-2 shRNA3 and shRNA4 were used for all subsequent experiments. Cellular growth of ovarian cancer cell, A10, showed a significant reduction in cellular proliferation post 48 h with shRNA3 and shRNA4 (46.23%, *P = 0.0051*, shRNA3 and 38.71%, *P = 0.0043*, shRNA4) and 72 h (30%, *P*
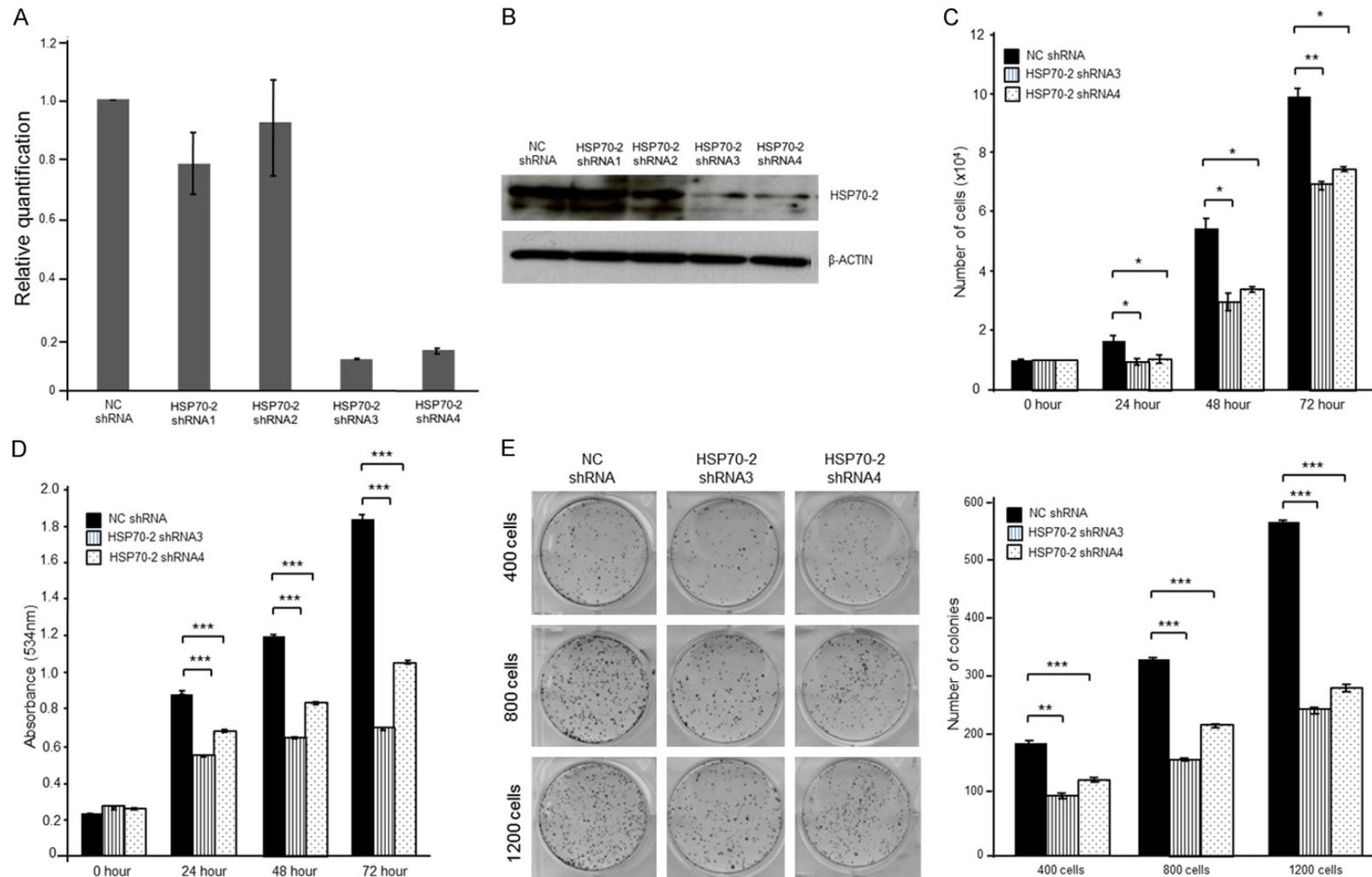
Figure 2. Ablation of HSP70-2 alters the malignant properties of ovarian cancer cell, A10. A. Bar diagram depicts qPCR data of all four HSP70-2 shRNA targets. B. Western blotting shows reduced HSP70-2 protein expression in shRNA3 and shRNA4 transfected cells as compared to NC shRNA, shRNA1 and shRNA2 transfected cells. C. Histogram demonstrates reduced cellular proliferation in cells transfected with shRNA3 and shRNA4 as compared to cells transfected with NC shRNA. D. Histogram depicts decreased cell viability by MTT assay in cells transfected with shRNA3 and shRNA4 as compared to cells transfected with NC shRNA. E. Representative images and histogram show the significant difference in number of colonies formed in cells transfected with shRNA3 and shRNA4 as compared to cells transfected with NC shRNA. The experiments were performed three independent times in triplicates. Data are represented as mean ± standard error of the mean. *$P<0.05$, **$P<0.001$, ***$P<0.0001$.
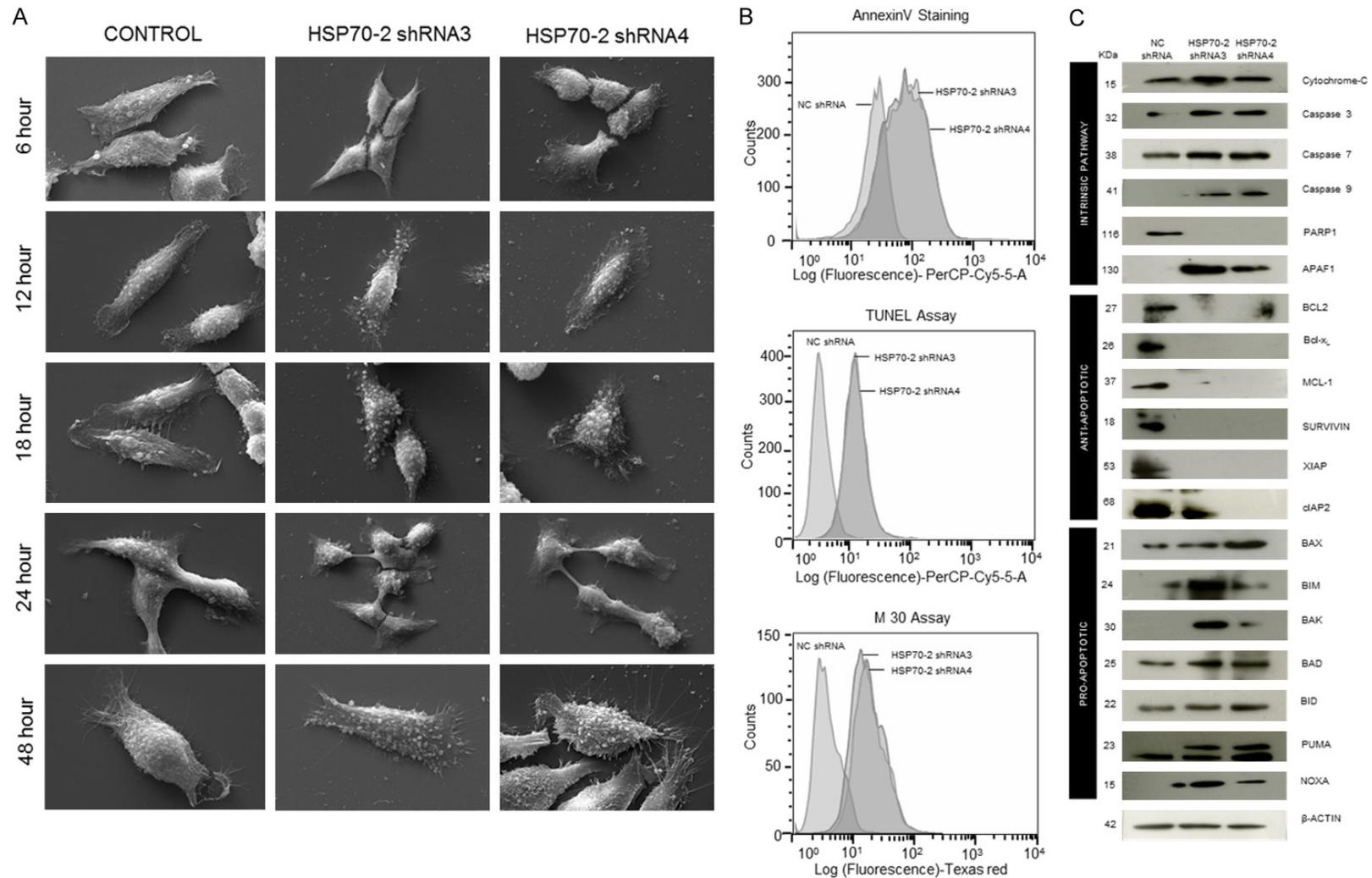
Figure 3. HSP70-2 ablation initiates apoptosis. A. Representative SEM images show no phenotypic changes in cells treated with NC shRNA. Initiation of membrane blebbing and apoptotic bodies formation is observed in cells treated with shRNA3 and shRNA4 after 12 hours which increased by 48 hours. Magnification: ×6000, WD = 6 mm, EHT = 20.00 kV. B. FACS analysis depicts increased percentage of cells expressing annexin V, BrdU and M30 on cell surface when transfected with shRNA3 and shRNA4 as compared to NC shRNA transfected cells. C. Western blot analysis shows upregulation of intrinsic pathway and pro-apoptotic molecules, while, downregulation of anti-apoptotic molecules. β-actin was used as a loading control. The experiments were performed three independent times in triplicates.

= *0.0007*, shRNA3 and 24.2%, *P = 0.0013*, shRNA4) as compared to NC shRNA (**Figure 2C**). Cellular viability assay also demonstrated significant reduction (*P<0.0001*) in percentage of viable cells transfected with shRNA3 [39.32% (24 h), 46.67% (48 h) and 62.16% (72 h)] and shRNA4 [24.72% (24 h), 30% (48 h) and 42.7% (72 h)] as compared to NC shRNA transfected cells (**Figure 2D**). Importantly, the clonogenic potential of ovarian cancer cells was significantly reduced (*P<0.0001*) when cells were transfected with shRNA3 (48-57% for 400-1200 cells per well) and shRNA4 (33-51% for 400-1200 cells per well) as compared to NC shRNA (**Figure 2E**).

Ablation of HSP70-2 initiates apoptosis

In order to study the effect of HSP70-2 protein ablation on phenotypic changes, ovarian cells were transfected with HSP70-2 shRNA3 and shRNA4 and subjected to scanning electron microscopy (SEM). The SEM images depicted no phenotypic changes in NC shRNA treated cells till 48 h, while cells transfected with shRNA3 and shRNA4 showed initiation of membrane blebbing and presence of apoptotic bodies after 12 h of treatment which continued and increased by 48 hours (**Figure 3A**). Lipofectamine, negative control, did not show any changes, however, DMSO and Paclitaxel, positive controls, showed drastic phenotypic changes even after 6 h of treatment (Supplementary Figure 1). Biochemical changes due to shRNA3 and shRNA4 were also assessed. Phosphatidyl serine translocation to the surface of cells was assessed by Annexin-V-PerCP-Cy5-5-A assay. Flow cytometric data showed that 48.9% and 58.4% of cells transfected with shRNA3 and shRNA4 expressed annexin-V on cell surface as compared to 0.97% cells transfected with NC shRNA (**Figure 3B**). In order to assess the onset of apoptosis, DNA fragmentation post transfection with shRNA3 and shRNA4 was assessed by TUNEL assay. Our results showed 61.2% and 64.5% of cells transfected with shRNA3 and shRNA4 respectively were found positive for BrdU staining as compared to 1.35% of cells transfected with NC shRNA (**Figure 3B**). In order to investigate the onset of intrinsic apoptosis pathway, M30 assay was performed to estimate caspase 3 activation. FACS data demonstrated that 47.3% and 57.7% of shRNA3 and shRNA4 tra-

nsfected cells expressed M30 epitope as compared to 0.50% of NC shRNA transfected cells (**Figure 3B**).

In addition, the effect of *HSP70-2* gene silencing was investigated on various molecules involved in apoptosis at the gene level. Quantitative-PCR data showed upregulation of *caspase 3*, *caspase 7*, *caspase 9, APAF1*, *BAX* and *NOXA*, while, *PARP1, BCL-2, Bcl-x_L*, *MCL-1*, *Survivin*, *XIAP* and *cIAP2* were downregulated (Supplementary Figure 2A and Supplementary Table 4). Subsequently, Western blotting analysis corroborated qPCR findings and revealed upregulation of intrinsic pathway molecules such as; cytochrome-C, caspase 3, caspase 7, caspase 9 and APAF1. The pro-apoptotic molecules such as, BAX, BIM, BAK, BAD, BID, PUMA, NOXA were also upregulated while PARP1 and anti-apoptotic molecules like BCL-2, Bcl-x_L, MCL-1, Survivin, XIAP and cIAP2 were downregulated in shRNA3 and shRNA4 transfected cells as compared to NC shRNA (**Figure 3C**). Hence, our data suggest that HSP70-2 gene and protein ablation is involved in initiating the onset of apoptosis.

HSP70-2 shRNA treatment arrests cell cycle

Next we studied the effect of gene silencing on cellular growth. Our flow cytometric analysis data revealed the accumulation of ovarian cancer cells in G0-G1 stage (M1), 67.82% in shRNA3 and 68.23% in shRNA4 transfected cells as compared to 57.18% in NC shRNA transfected cells (**Figure 4A**). However, no significant difference was observed in percentage of cells in S-phase (M2) and G2-M phase [(M3); **Figure 4A**]. Further, various molecules involved in cell cycle were validated by qPCR which showed that cell cycle inhibitors, *p21* and *p27* were upregulated, whereas, *cyclin A2, cyclin B1, cyclin D1, cyclin E, CDK1, CDK2, CDK4* and *CDK6* were downregulated (Supplementary Figure 2B and Supplementary Table 2). Further, Western blot results supported our qPCR findings which showed upregulation of p16, p21, Rb, while downregulation of CDK1, CDK2, CDK4, CDK6, cyclin D1, cyclin E, cyclin A2, cyclin B1, phosphorylated-Rb (p-Rb) and E2F1 (**Figure 4B**). As a result of cell cycle arrest, cancer cell may enter into a phase of cellular senescence. Interestingly, an enhanced β-galactosidaseactivity which is an indicator of cel-
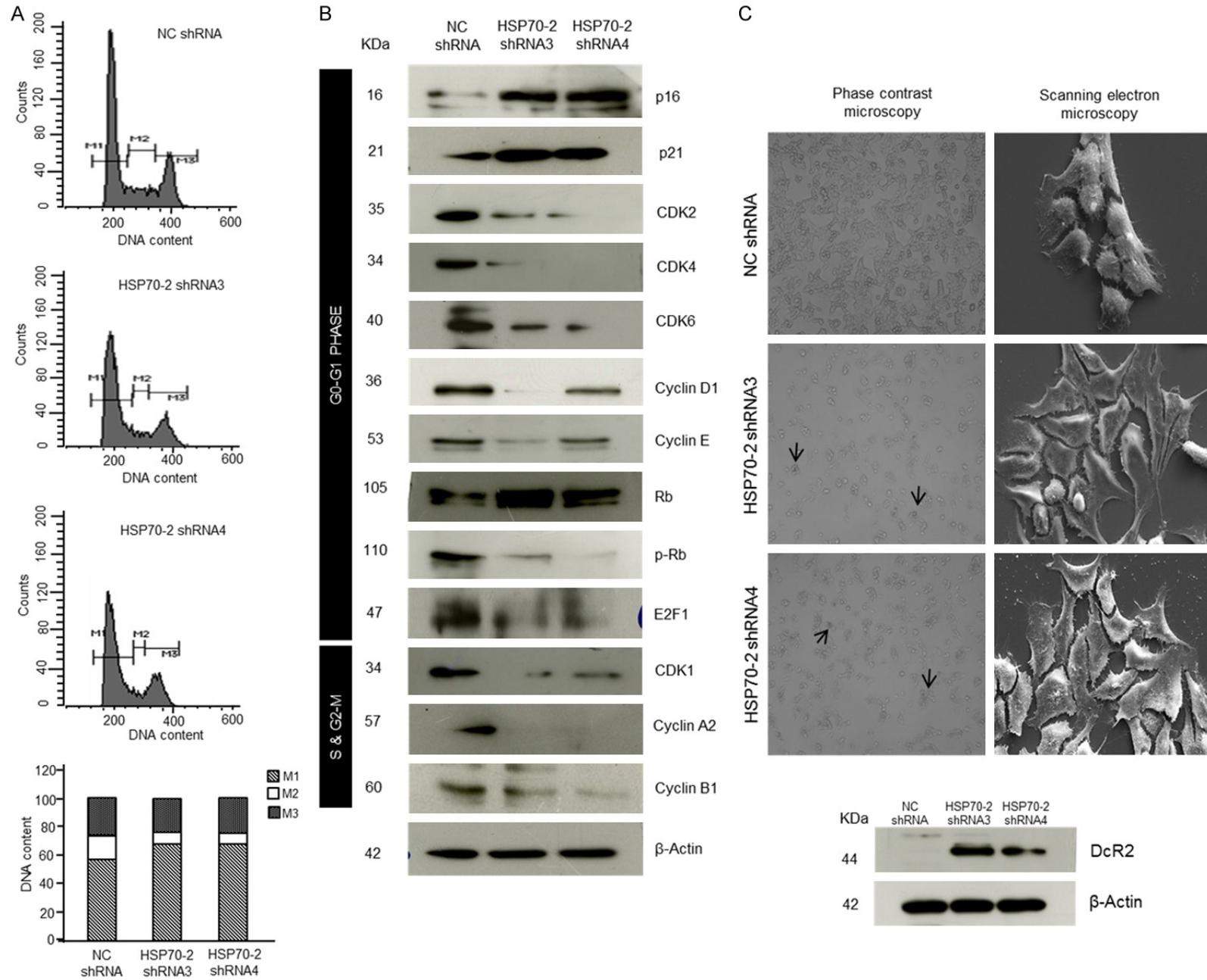
Figure 4. HSP70-2 shRNA treatment arrests cell growth. A. Flow cytometric analysis shows cell cycle analysis of NC shRNA, shRNA3 and shRNA4 transfected cells stained with PI (M1: G0-G1, M2: S and M3: G2-M phase). Bar diagram depicts cumulative percentage accumulation of cells in M1 (57.18%: NC shRNA, 67.82%: shRNA3, 68.23%: shRNA4), M2 (16.81%: NC shRNA, 8.49%: shRNA3, 6.75%: shRNA4) and M3 (25.65%: NC shRNA, 23.33%: shRNA3, 25.33%: shRNA4). B. Western blotting depicts the upregulation of p16, p21, Rb, while downregulation of cyclins, cyclin dependent kinases, p-Rb and E2F1. β-actin was used as a loading control. C. Representative phase contrast images show enhanced β-galactosidase activity (arrow) in shRNA3 and shRNA4 transfected cells. Representative SEM images show initiation of senescence in shRNA3 and shRNA4 transfected cells revealing flattened phenotypic characteristics. Western blotting shows increased DcR2 expression in shRNA3 and shRNA4 transfected cells. Phase contrast microscopy: Original magnification ×100, objective ×10. SEM: Magnification: ×6000, WD = 6 mm, EHT = 20.00 kV. The experiments were performed three independent times in triplicates.

lular senescence was observed in the cells transfected with shRNA3 and shRNA4 as compared to NC shRNA transfected cells (**Figure 4C**). In addition, SEM images were captured which further validated our data revealing flattening of cells in shRNA3 and shRNA4 transfected cells as compared to NC shRNA transfected cells (**Figure 4C**) suggesting cellular senescence state. Further, Western blot data also supported the phenotypic characteristics of cellular senescence wherein Decoy receptor 2 (DcR2), a marker for senescence onset was found to be upregulated in shRNA3 and shRNA4 transfected cells as compared to NC shRNA transfected cells (**Figure 4C**). Collectively, our data suggest that HSP70-2 shRNA treatment arrests the cell growth in G0-G1 stage and induces cellular senescence.

Knockdown of HSP70-2 inhibits cellular motility

Metastasis is a multistep process and was assessed by studying migration, invasion and cellular motility of ovarian cancer cells. Our cell migration assay revealed a significant reduction in cells migrating through insert membrane in shRNA3 (45.5%, *P<0.0001*) and shRNA4 (37.64%, *P<0.001*) transfected cells as compared to NC shRNA transfected cells (**Figure 5A**). Similarly, our invasion assay showed reduced number of shRNA3 (55.21%, *P<0.0001*) and shRNA4 (48.56%, *P<0.0001*) transfected cells invading through matrigel as compared to NC shRNA transfected cells (**Figure 5A**). Cellular motility was also assessed by wound healing assay which demonstrated the inhibition of cellular motility. HSP70-2 shRNA3 and shRNA4 transfected cells showed delayed wound healing ability as compared to NC shRNA transfected cells (**Figure 5B**). Relative wound healing index was found to be significantly higher for shRNA3 and shRNA4 transfected cells (*P<*

0.001) as compared to NC shRNA transfected cells after 24 hours of transfection (**Figure 5B**).

Next we studied the status of various molecules associated with migration, invasion and cellular motility. Various genes under investigation showed (Supplementary Figure 2C and Supplementary Table 2) the relative quantification of various mesenchymal marker genes such as; *N-cadherin*, *SNAIL*, *SLUG*, *VIMENTIN*, *SMA*, *MMP2*, *MMP3*, *MMP9* and *TWIST* in cells transfected with shRNA3 and shRNA4. In order to validate gene expression data at the protein level, Western blotting was carried out. Epithelial markers, such as E-cadherin, cytokeratin 18 and EMA were upregulated while, mesenchymal markers, N-cadherin, SNAIL, SLUG, VIMENTIN, SMA, MMP2, MMP3, MMP9 and TWIST were downregulated (**Figure 5C**). Our study clearly indicates that HSP70-2 ablation inhibits migratory, invasive and cellular motility ability of ovarian cancer cells by altering the key molecules involved in various metastatic processes.

HSP70-2 knockdown retards growth of the human ovarian xenografts in in-vivo mouse model

For *in-vivo* studies, the ovarian human xenograft was established in immunocompromised SCID mice treated with HSP70-2 shRNA3. There was a significant reduction (*P* = 0.0015) in tumor size and tumor volume of shRNA3 treated mice as compared to those treated with NC shRNA (**Figure 6A**, **6B**). Moreover, significant survival (*P = 0.037*) was observed in mice treated with HSP70-2 shRNA3 as compared to NC shRNA (**Figure 6C**). Further, qPCR and Western blot analysis showed a significant reduction (*P* = 0.003) in *HSP70-2* mRNA (50%) (**Figure 6D**) and protein expression (**Figure 6D**) in tumor specimens treated with shRNA3 as compared to NC shRNA. In addition, immuno-
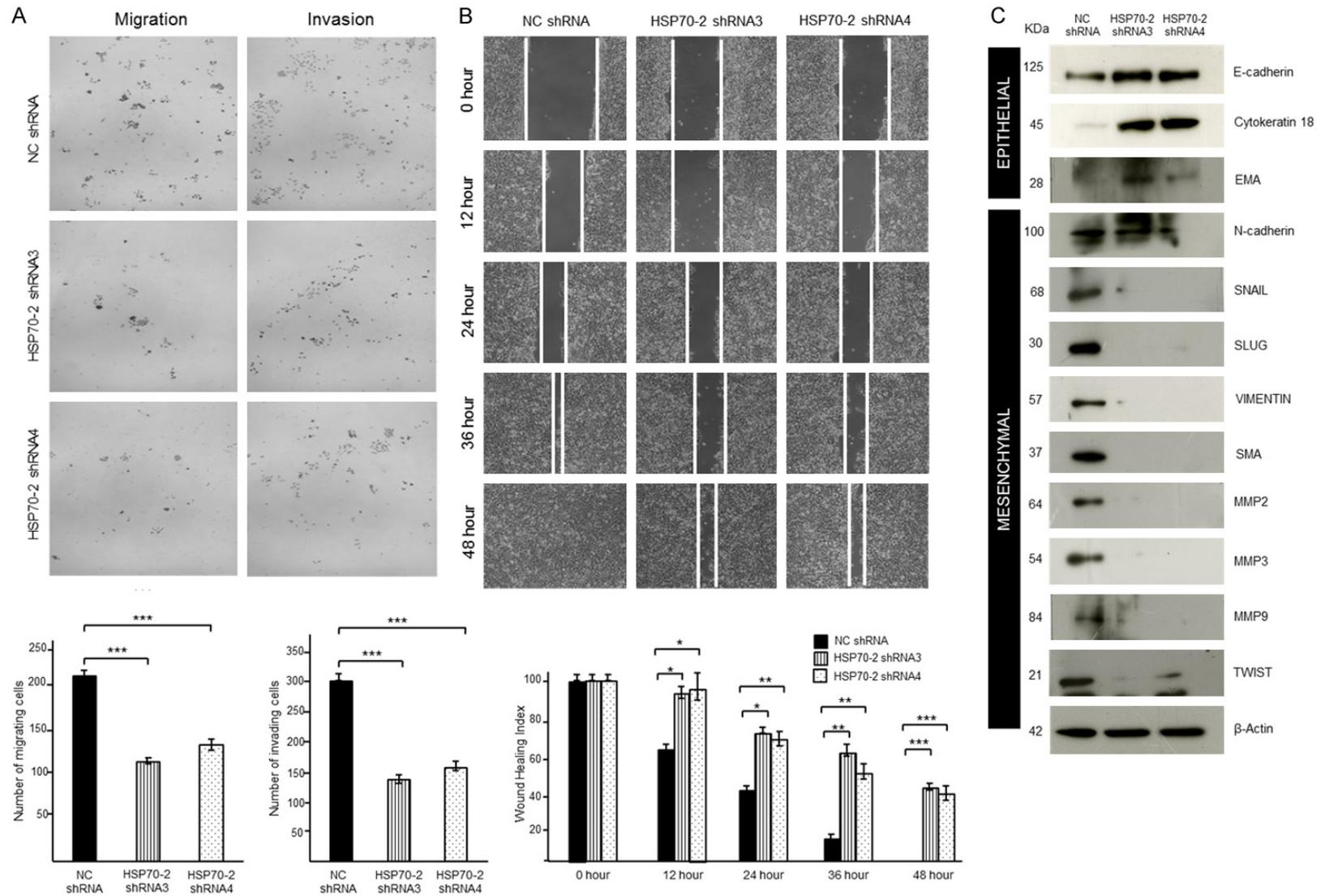
Figure 5. HSP70-2 ablation inhibits cellular motility. A. Phase contrast images and histogram show the significant difference in migration or invasion abilities through insert membrane and matrigel in shRNA3 and shRNA4 transfected cells respectively as compared to NC shRNA transfected cells. B. Representative images show delayed wound healing in shRNA3 and shRNA4 transfected cells as compared to NC shRNA transfected cells from 12-48 hours. Histogram depicts relative wound healing index at different time points. C. Western blot analysis shows the upregulation of epithelial markers, while downregulation of mesenchymal markers. Original magnification ×100, objective ×10. The experiments were performed three independent times in triplicates. Data are represented as mean ± standard error of the mean. *$P<0.05$, **$P<0.001$, ***$P<0.0001$.
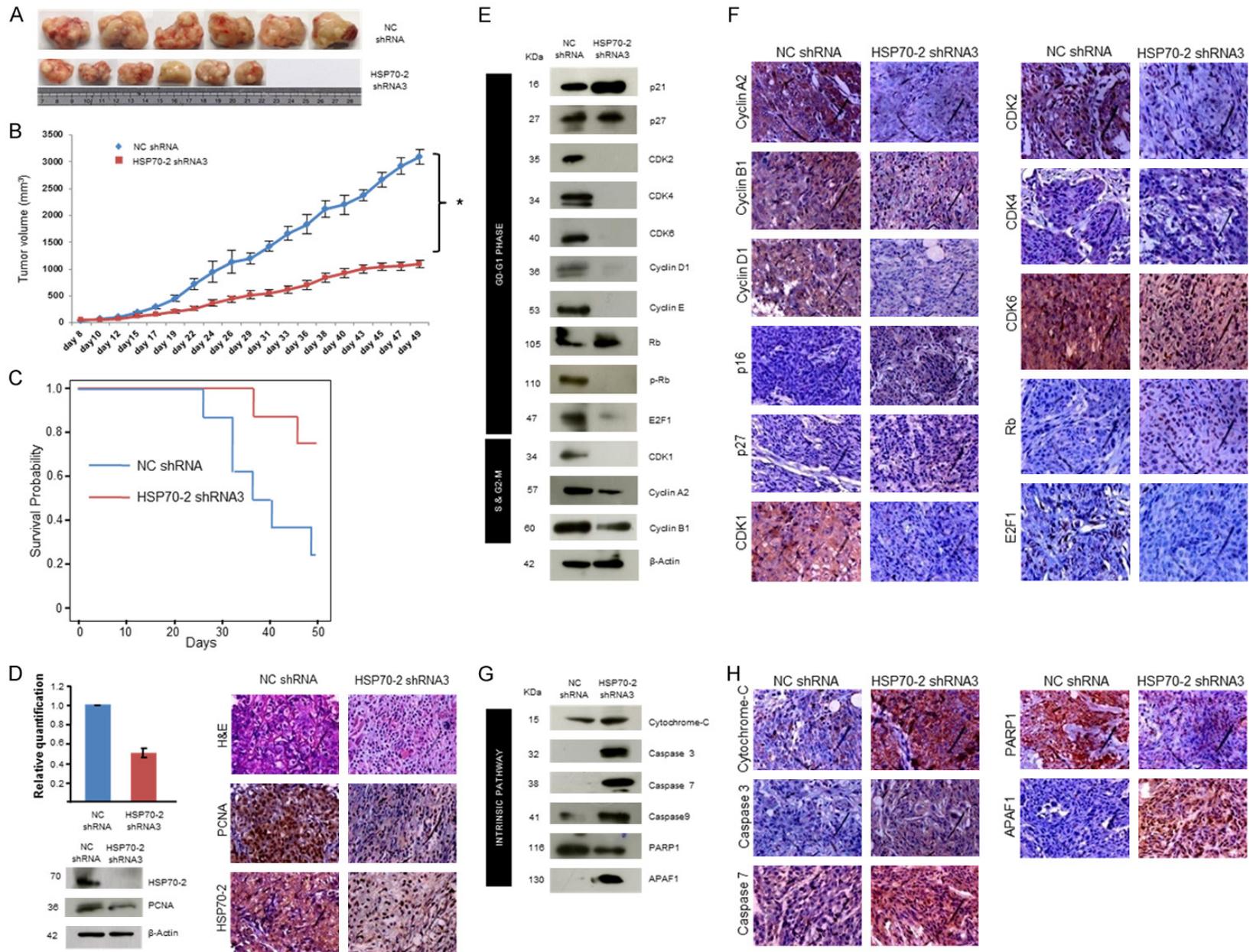
Figure 6. HSP70-2 ablation retards tumor growth *in-vivo* human xenograft mouse model. A. Representative images show the difference in tumor dissected and compared on scale shows reduced tumor size when treated with shRNA3 as compared to NC shRNA treated mice. B. Line graph depicts the significant difference in the tumor volume of shRNA3 treated mice as compared to NC shRNA treated mice *P<0.0001*. C. Kaplan-Meier graph shows significant survival in mice treated with HSP70-2 shRNA3 as compared to NC shRNA, *P = 0.037* by log-rank test. D. Histogram shows qPCR results showing *HSP70-2* gene downregulation in tumor treated with shRNA3 as compared to NC shRNA treatment. Western blot analysis on tumor lysates prepared from tumor retrieved from SCID mice shows reduced expression of HSP70-2 and PCNA in shRNA3 treated mice as compared to NC shRNA treated mice. β-actin was used as a loading control. Representative images of IHC analysis on the serial sections of tumor reveals reduced expression of PCNA and HSP70-2 in shRNA3 treated mice as compared to NC shRNA treated mice. The top panel shows the cytostructure by H and E staining. E. Western blot analysis of tumor lysates depicts effect of knockdown of HSP70-2 on various molecules of cell cycle. F. Representative IHC images show reduced immuno-reactivity of cyclin A2, cyclin B1, cyclin D1, CDK1, CDK2, CDK4, CDK6 and E2F1 and increased immuno-reactivity of p21, p27 and Rb in serial sections of tumor obtained from shRNA3 treated mice as compared to NC shRNA treated mice. G. Protein validation by Western blotting carried out in tumor lysates demonstrates upregulation of intrinsic pathway molecules and downregulation of PARP1. H. IHC analysis on serial sections of tumor shows increased immuno-reactivity of intrinsic pathway molecules. Original magnification ×400, objective ×40. Data are represented as mean ± standard error of the mean.

histochemical (IHC) analysis of xenograft tumor specimens validated these results and showed reduced expression of HSP70-2 and PCNA (proliferating cell nuclear antigen) in the shRNA3 treated tumors as compared to NC shRNA treated tumors (**Figure 6D**).

Next, we validated our *in-vitro* findings of cell cycle regulators in the xenograft model system. As expected there was a marked reduction in the gene expression of *cyclin A2, CDK1, CDK2, CDK4, CDK6* and *E2F1*, whereas, increased expression of *p21, p27* and *Rb* was observed in shRNA3 treated mice as compared to NC shRNA treated mice (Supplementary Figure 3A and Supplementary Table 3). Further, Western blot analysis confirmed these observations and showed upregulation of cell cycle inhibitors, p21 and p27 and tumor suppressor, Rb. As expected, cyclin A2, cyclin B1, cyclin D1, cyclin E and cyclin dependent kinases like CDK1, CDK2, CDK4 and CDK6 and p-Rb and E2F1 were downregulated (**Figure 6E**). The paraffin embedded tumor serial sections were subjected to IHC to validate the gene and protein expression data of tumor lysates. IHC images showed reduced immuno-reactivity of cyclin A2, cyclin B1, cyclin D1, CDK1, CDK2, CDK4, CDK6 and E2F1, while, increased immuno-reactivity of p16, p27 and Rb in shRNA3 treated tumor as compared to NC shRNA treated tumor (**Figure 6F**).

The effect of HSP70-2 shRNA3 treatment was also studied on various molecules of apoptotic pathway in these xenograft tumor specimens. Quantitative-PCR analysis of tumor specimens depicted upregulation of *cytochrome-C, cas-*

pase 3, caspase 7, caspase 9, APAF1, BAX and *NOXA*, while, downregulation of *BCL-2, Bcl-x_L, MCL-1* and *XIAP* in shRNA3 treated tumor as compared to NC shRNA treated tumor (Supplementary Figure 3B and Supplementary Table 3). Western blot analysis on tumor specimen lysates confirmed the upregulation of intrinsic pathway molecules, such as cytochrome-C, caspase 3, caspase 7, caspase 9, APAF1 and pro-apoptotic molecules like BAX, BIM, BAK, BAD, BID, PUMA and NOXA while, PARP1 and anti-apoptotic molecules like BCL-2, Bcl-x_L, MCL-1, Survivin, XIAP and cIAP2 were downregulated (**Figures 6G**, **7A**) in shRNA3 treated animals. Our IHC studies on tumor serial sections validated the qPCR and protein expression results of tumor lysate. These results showed increased immuno-reactivity of cytochrome-C, caspase 3, caspase 7, APAF1 and pro-apoptotic molecules like BAX, BIM, BAK, BID and NOXA were upregulated while, PARP1 and anti-apoptotic molecules like BCL-2, Bcl-x_L, MCL-1, Survivin, XIAP and cIAP2 showed reduced immuno-reactivity (**Figures 6H**, **7B**).

Various key molecules involved in the EMT were further analyzed. Our qPCR data revealed the upregulation of epithelial markers, *E-cadherin, cytokeratin 18* and *EMA* in the shRNA3 treated tumors as compared to NC shRNA treated tumors. Further there was downregulation of mesenchymal markers, *N-cadherin, SNAIL, SLUG, VIMENTIN, SMA, MMP2, MMP3, MMP9* and *TWIST* in the shRNA3 treated tumors as compared to NC shRNA treated tumors (Supplementary Figure 3C and Supplementary
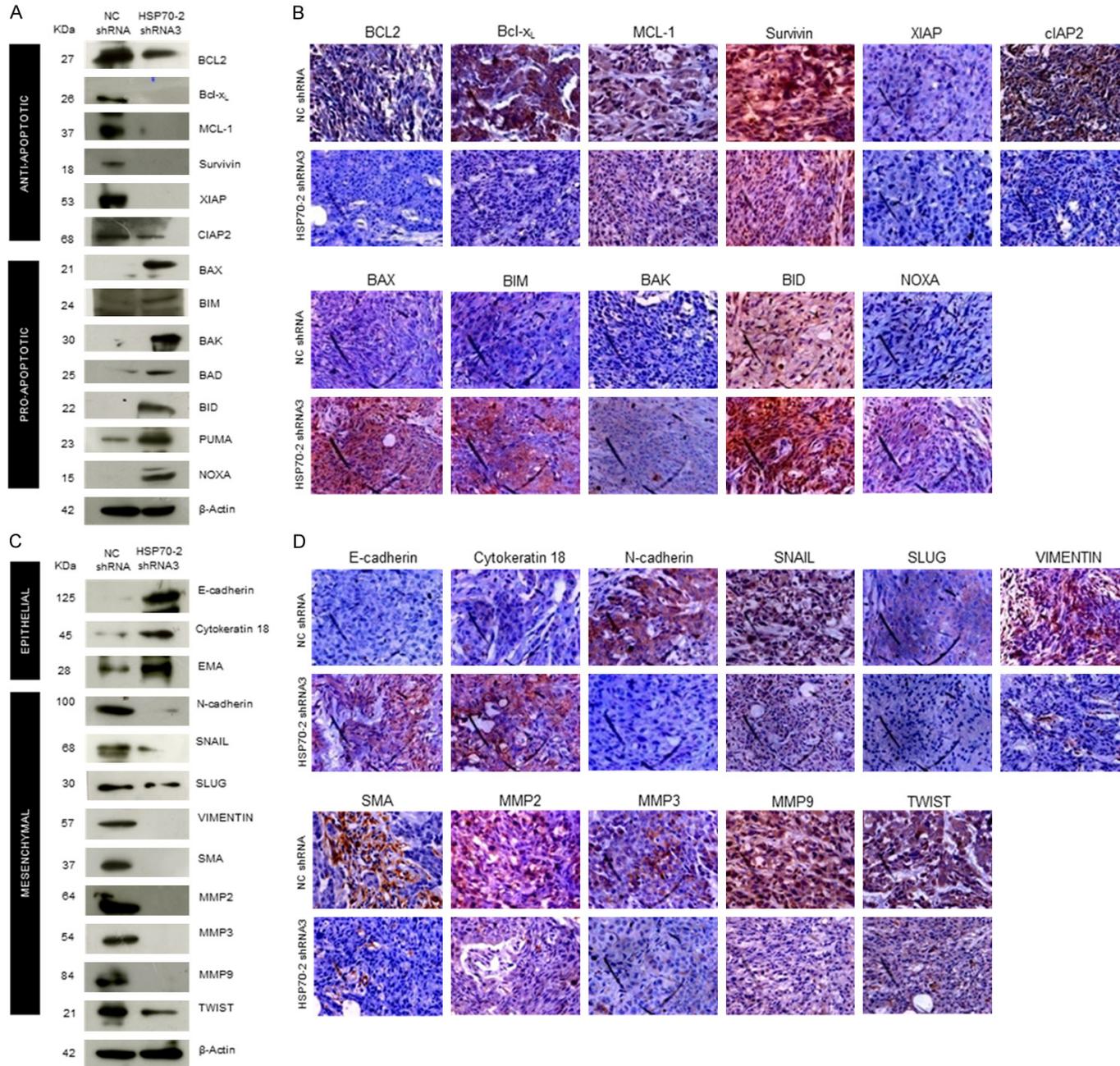
Figure 7. HSP70-2 shRNA treatment initiates the onset of apoptosis and inhibits EMT in tumor cells. A. Western blot data show upregulation of pro-apoptotic molecules and downregulation of anti-apoptotic molecules. B. Representative images of IHC of serial sections exhibit increased immuno-reactivity of pro-apoptotic molecules in shRNA3 treated mice as compared to NC shRNA treated mice. However, decreased immuno-reactivity is observed in case of anti-apoptotic molecules. C. Western blotting in tumor lysates shows upregulation of epithelial markers and downregulation of mesenchymal markers in tumor cells treated with shRNA3 as compared to NC shRNA. D. Representative micrographs of IHC analysis on serial tumor sections shows increased immuno-reactivity of epithelial markers and reduced immuno-reactivity of mesenchymal markers in shRNA3 treated mice as compared to NC shRNA treated mice. Original magnification ×400, objective ×40.

Table 3). Further, the Western blot analysis of tumor xenograft lysate treated with shRNA3 confirmed the qPCR findings and revealed that E-cadherin, cytokeratin 18 and EMA were upregulated whereas downregulation of N-cadherin, SNAIL, SLUG, VIMENTIN, SMA, MMP2, MMP3, MMP9 and TWIST was observed (**Figure 7C**). Validation for qPCR and Western blotting results were further confirmed by IHC which showed that immuno-reactivity of E-cadherin and cytokeratin 18 was increased, while decreased immuno-reactivity of N-cadherin, SNAIL, SLUG, VIMENTIN, SMA, MMP2, MMP3, MMP9 and TWIST was observed in shRNA3 treated tumor as compared to NC shRNA treated tumor (**Figure 7D**).

Discussion

Ovarian cancer is one of the most common cancer amongst gynecological cancers [1]. Especially serous ovarian carcinoma is the most prevalent subtype of epithelial ovarian cancer (EOC) and accounts for about 80-90% of all ovarian cancers [3]. Early-stage ovarian cancers are normally asymptomatic and hence are diagnosed at an advanced disease stage, when treatment modalities are limited [15]. Till date few cancer testis (CT) antigens expression have been shown to be associated with ovarian cancer [16-19] however, none of these CT antigens are in clinical practice yet. In this study, we investigated the role of HSP70-2 in EOC and found its expression in all the EOC cell lines. Small interfering RNA-mediated (shRNA) knockdown of HSP70-2 expression in EOC cells resulted in reduced cellular proliferation, cell viability, colony forming ability, cellular motility, invasion ability and retarded tumor growth in *in-vivo* ovarian cancer xenograft mouse model. Our recent studies also demonstrated that ectopic expression HSP70-2 does promote cellular proliferation, migration and invasion in *in vitro* and tumor growth in *in vivo* in bladder cancer [7], cervix cancer [8], breast cancer [9] and

colorectal cancer [10]. Recently, it has been reported [20] that employing shRNA approach to silence genes involved in disease progression may be a novel approach for development of a new class of therapeutics.

In an attempt for developing a novel therapeutic target for ovarian cancer, our study demonstrated that HSP70-2 depleted cells showed downregulation of anti-apoptotic proteins and increased expression of pro-apoptotic genes. This in turn further led to upregulation of cytochrome-C, caspase 3, caspase 7 and caspase 9. Also, Apoptotic protease activating factor 1 (APAF1) was found to be upregulated resulting in reduced cellular growth and hence the cell death. Similarly, recent studies also showed that anti-apoptotic gene BCL-2 along with other members, Bcl-x$_L$ and MCL-1 suppress the activity of pro-apoptotic proteins BAX and BAK [21]. In the absence of anti-apoptotic genes, BAX and BAK disrupt the integrity of the outer mitochondrial membrane, causing the release of pro-apoptotic signaling protein, cytochrome-C, which in turn activates the cascade of caspases leading to multiple cellular changes associated with apoptosis [21]. Further in support of our data, yet another study has shown that gene silencing of c-myc (proto-oncogene) led to upregulation of apoptotic-related molecules caspase 3, caspase 9 and PARP1 in ovarian cancer cells [22]. Our investigation distinctly show that HSP70-2 promotes cellular growth and thus, depletion of HSP70-2 seems to promote apoptosis in ovarian cancer cells.

Cell cycle dysregulation is a common molecular finding with upregulation of cyclin D1 or E1, E2F1 or cyclin dependent kinases (CDK2), and downregulation of CDK inhibitors (p16, p21 and p27) have been observed in ovarian cancer [23]. Interestingly, our findings revealed that HSP70-2 depleted cells had increased expression of cell cycle inhibitors (p16, p21) which in turn downregulated the expression of cyclin D,

cyclin E thus resulting in cell growth arrest (**Figure 4**). As a result, downregulation of CDK4/6-cyclin D or CDK2-cyclin E, decreased phosphorylation of Rb was found which further lead to increased expression of E2F1 and hence, arrest of cancer cells at G0-G1 phase of cell cycle. These findings were similar to earlier studies carried out on salt-inducible kinase 3 [24] and COX-1 [25] in ovarian cancer cells. Hence, ablation of HSP70-2 arrests the cell cycle and inhibited cellular growth of ovarian cancer cells.

EOC cells display an aggressive characteristic feature which has the ability to migrate and invade into the peritoneal cavity and metastasize to local organs [26]. Our study revealed that HSP70-2 depleted cells had reduced migratory and invasive ability indicating that HSP70-2 plays an important role in cellular motility. E-cadherin helps to assemble epithelial cells and maintain structural integrity and loss of E-cadherin is considered to be the main alteration in the cancer cells. Moreover, reduction of E-cadherin expression has been shown to be associated with invasion and metastasis [23]. Contrary to this, adhesion molecule, N-cadherin is often upregulated and is associated with the cell migration and invasion in cancer cells [21]. Transcriptional factors, including SNAIL, SLUG and TWIST involved in EMT have been found to be expressed in various malignancies [23]. These studies suggested that expression of transcription factors lead to loss of adherent junctions, associated conversion from epithelial to spindle morphology, expression of matrix degrading enzymes (MMP's) and increased motility [21]. Interestingly, our data also showed similar finding at molecular level, wherein, HSP70-2 ablated cells had increased expression of epithelial markers including, E-cadherin, while downregulation of mesenchymal markers, N-cadherin, VIMENTIN, SMA, MMP2, MMP3 and MMP9. Transcription factors such as SNAIL, SLUG and TWIST which promotes EMT were also down-regulated (**Figure 5**). Other studies have also shown in ovarian cancer cells that COX-1 depleted cells show reduced expression of genes promoting cell invasion or migration [23]. We are the first to report that CT antigen, HSP70-2 depleted ovarian cancer cells have reduced cellular motility as a result of low expression of EMT molecules.

Encouraged by our observations in cell culture, we confirmed these findings in *in-vivo* mouse model. Animals treated with HSP70-2 shRNA exhibited retarded tumor growth which was consistent with our previous findings in bladder and cervix cancer xenograft mouse model [7, 8]. Our data further showed that HSP70-2 shRNA treatment altered various genes of cell cycle in G0-G1 stage which resulted in cell cycle arrest and caused senescence. Other studies on COX-2 selective inhibitor [27] and metformin (antidiabetic drug [28]) supported our data and showed that these inhibitors led to downregulation of cyclin D1 as assessed by IHC in *in-vivo* ovarian cancer system. So far no CT antigen has been explored for its involvement at molecular level in various pathways contributing towards tumor growth and cellular motility in ovarian cancer cells. Apparently, this seems to be the first report showing role of HSP70-2 in cellular growth in the ovarian cancer cells. Apoptosis is one such physiological process by which tumor growth can be retarded. We showed the effect of HSP70-2 knockdown on tumor regression in *in-vivo* mouse model and found that HSP70-2 depleted tumor had increased expression of cytochrome-C, caspases, pro-apoptotic molecules, while decreased expression of anti-apoptotic molecules at both mRNA as well as protein levels. Some earlier studies have also shown similar trend in tumor regression treated with NCX-4016, a nitro-derivative of aspirin [29] and RY-2f, an isoflavone analog [30] in human ovarian cancer xenograft model. Thus, HSP70-2 seems to be a key molecule involved in growth and motility of ovarian cancer cells.

HSP70-2 is member of HSP70 family of proteins [6]. HSP70 proteins can be thought of as a potent buffering system for cellular stress, either from extrinsic (physiological, viral and environmental) or intrinsic (replicative or oncogenic) stimuli. HSP70-2 protein may have a buffering system in ovarian cancer cells and may utilize this property to stabilize the proteins that are required for ovarian cancer cell survival. Therefore, future studies are warranted to target the HSP70-2 as combination therapy to treat the ovarian cancer patients. Recently it was documented that gene silencing of CDK11 increased the cytotoxic effect of chemotherapeutic agent paclitaxel in ovarian cancer cells [31]. The antitumor effect of HSP70-2

knockdown has paved a way for exploring shRNA based novel cancer treatment. In this context, as monotherapy, recent clinical trials employing siRNAs against VEGF and kinesin spindle protein (KSP) have shown promising results to treat metastatic endometrial and hepatocellular carcinoma [20] as a new therapeutic treatment modality for cancer.

Collectively, our study shows that HSP70-2 plays an important role in ovarian cancer. Gene silencing studies clearly indicate that HSP70-2 promotes cellular growth and multistep process including migration and invasion of ovarian cancer cells. Hence, our study suggests that HSP70-2 may be a putative therapeutic target in combination with other chemotherapeutic agents against ovarian cancer for future treatment strategies and warrants future studies.

Acknowledgements

Disclosure of conflict of interest

None.

Address correspondence to: Anil Suri, Cancer Research Program, Cancer Microarray, Genes and Proteins Laboratory, National Institute of Immunology, ArunaAsaf Ali Marg, New Delhi 110067, India. Tel: 91-11-26703-700; Fax: 91-11-26-1621-25; 91-11-26742125; E-mail: anil@nii.res.in

References

[1] Siegel RL, Miller KD, Jemal A. Cancer statistics. CA Cancer J Clin 2015; 65: 5-29.

[2] Rauh-Hain JA, Krivak TC, DelCarmen MG, Olawaiye AB. Ovarian cancer screening and early detection in the general population. Rev Obstet Gynecol 2011; 4: 15-21.

[3] Nolen B, Marrangoni A, Velikokhatnaya L, Prosser D, Winans M, Gorelik E, Lokshin A. A serum based analysis of ovarian epithelial tumourigenesis. Gynecol Oncol 2009; 112: 47-54.

[4] Gjerstorff MF, Andersen MH, Ditzel HJ. Oncogenic cancer/testis antigens: prime candidates for immunotherapy. Oncotarget 2015; 6: 15772-15787.

[5] Suri A, Saini S, Sinha A, Agarwal S, Verma A, Parashar D, Singh S, Gupta N, Jagadish N. Cancer testis antigens: a new paradigm for cancer therapy. Oncoimmunology 2012; 1: 1194-6.

[6] Rohde M, Daugaard M, Jensen MH, Helin K, Nylandsted J, Jäättelä M. Members of the heat-shock protein 70 family promote cancer cell growth by distinct mechanisms. Genes Dev 2005; 19: 570-582.

[7] Garg M, Kanojia D, Seth A, Kumar R, Gupta A, Surolia A, Suri A. Heat-shock protein 70-2 (HSP70-2) expression in bladder urothelial carcinoma is associated with tumor progression and promotes migration and invasion. Eur J Cancer 2010; 46: 207-215.

[8] Garg M, Kanojia D, Saini S, Suri S, Gupta A, Surolia A, Suri A. Germ cell-specific heat shock protein 70-2 is expressed in cervical carcinoma and is involved in the growth, migration, and invasion of cervical cells. Cancer 2010; 116: 3785-3796.

[9] Jagadish N, Agarwal S, Gupta N, Fatima R, Devi S, Kumar V, Suri V, Kumar R, Suri V, Sadasukhi TC, Gupta A, Ansari AS, Lohiya NK, Suri A. Heat shock protein 70-2 (HSP70-2) overexpression in breast cancer. J Exp Clin Cancer Res 2016; 35: 150.

[10] Jagadish N, Parashar D, Gupta N, Agarwal S, Suri V, Kumar R, Suri V, Sadasukhi TC, Gupta A, Ansari AS, Lohiya NK, Suri A. Heat shock protein 70-2 (HSP70-2) is a novel therapeutic target for colorectal cancer and is associated with tumor growth. BMC Cancer 2016; 16: 561.

[11] Singh S, Suri A. Targeting the testis-specific heat-shock protein 70-2 (HSP70-2) reduces cellular growth, migration, and invasion in renal cell carcinoma cells. Tumor Biol 2014; 35: 12695-12706.

[12] Zhu D, Dix DJ, Eddy EM. HSP70-2 is required for CDC2 kinase activity in meiosis I of mouse spermatocytes. Development 1997; 124: 3007-3014.

[13] Eddy EM. Role of heat shock protein HSP70-2 in spermatogenesis. Rev Reprod 1999; 4: 23-30.

[14] Jagadish N, Parashar D, Gupta N, Agarwal S, Purohit S, Kumar V, Sharma A, Fatima R, Topno AP, Shaha C, Suri A. A-kinase anchor protein 4 (AKAP4) a promising therapeutic target of

colorectal cancer. J Exp Clin Cancer Res 2015; 34: 142.

[15] Romero I, Bast RC Jr. Minireview: Human Ovarian Cancer: Biology, Current Management, and Paths to Personalizing Therapy. Endocrinology 2012; 153: 1593-602.

[16] Agarwal S, Saini S, Parashar D, Verma A, Sinha A, Jagadish N, Batra A, Suri S, Gupta A, Ansari AS, Lohiya NK, Suri A. The novel cancer-testis antigen A-kinase anchor protein 4 (AKAP4) is a potential target for immunotherapy of ovarian serous carcinoma. Oncoimmunology 2013; 2: e24270.

[17] Odunsi K, Jungbluth AA, Stockert E, Qian F, Gnjatic S, Tammela J, Intengan M, Beck A, Keitz B, Santiago D, Williamson B, Scanlan MJ, Ritter G, Chen YT, Driscoll D, Sood A, Lele S, Old LJ. NY-ESO-1 and LAGE-1 cancer-testis antigens are potential targets for immunotherapy in epithelial ovarian cancer. Cancer Res 2003; 63: 6076-6083.

[18] Tammela J, Uenaka A, Ono T, Noguchi Y, Jungbluth AA, Mhawech-Fauceglia P, Qian F, Schneider S, Sharma S, Driscoll D, Lele S, Old LJ, Nakayama E, Odunsi K. OY-TES-1 expression and serum immune-reactivity in epithelial ovarian cancer. Int J Oncol 2006; 29: 903-910.

[19] Garg M, Chaurasiya D, Rana R, Jagadish N, Kanojia D, Dudha N, Kamran N, Salhan S, Bhatnagar A, Suri S, Gupta A, Suri A. Sperm-associated antigen 9, a novel cancer testis antigen, is a potential target for immunotherapy in epithelial ovarian cancer. Clin Cancer Res 2007; 13: 1421-1428.

[20] Tabernero J, Shapiro GI, LoRusso PM, Cervantes A, Schwartz GK, Weiss GJ, Paz-Ares L, Cho DC, Infante JR, Alsina M, Gounder MM, Falzone R, Harrop J, White AC, Toudjarska I, Bumcrot D, Meyers RE, Hinkle G, Svrzikapa N, Hutabarat RM, Clausen VA, Cehelsky J, Nochur SV, Gamba-Vitalo C, Vaishnaw AK, Sah DW, Gollob JA, Burris HA 3rd. First-in humans trial of an RNA interference therapeutic targeting VEGF and KSP in cancer patients with liver involvement. Cancer Discov 2013; 3: 406-417.

[21] Hanahan D, Weinberg RA. Review hallmarks of cancer: The next generation. Cell 2011; 144: 646-674.

[22] Reyes-Gonzalez JM, Armaiz-Pena GN, Mangala LS, Valiyeva F, Ivan C, Pradeep S, Echevarría-Vargas IM, Rivera-Reyes A, Sood AK, Vivas-Mejía PE. Targeting c-MYC in platinum-resistant ovarian cancer. Mol Cancer Ther 2015; 14: 2260-2269.

[23] Konecny GE, Winterhoff B, Kolarova T, Qi J, Manivong K, Dering J, Yang G, Chalukya M, Wang HJ, Anderson L, Kalli KR, Finn RS, Ginther C, Jones S, Velculescu VE, Riehle D, Cliby WA, Randolph S, Koehler M, Hartmann LC, Slamon DJ. Expression of p16 and retinoblastoma determines response to CDK4/6 inhibition in ovarian cancer. Clin Cancer Res 2011; 17: 1591-1602.

[24] Charoenfuprasert S, Yang YY, Lee YC, Chao KC, Chu PY, Lai CR, Hsu KF, Chang KC, Chen YC, Chen LT, Chang JY, Leu SJ, Shih NY. Identification of salt-inducible kinase 3 as a novel tumor antigen associated with tumorigenesis of ovarian cancer. Oncogene 2011; 30: 3570-3584.

[25] Wilson AJ, Fadare O, Beeghly-Fadiel A, Son DS, Liu Q, Zhao S, Saskowski J, Uddin MJ, Daniel C, Crews B, Lehmann BD, Pietenpol JA, Crispens MA, Marnett LJ, Khabele D. Aberrant over-expression of COX-1 intersects multiple pro-tumorigenic pathways in high-grade serous ovarian cancer. Oncotarget 2015; 6: 21353-21368.

[26] Lokman NA, Elder ASF, Ween MP, Pyragius CE, Hoffmann P, Oehler MK, Ricciardelli C. Annexin A2 is regulated by ovarian cancer-peritoneal cell interactions and promotes metastasis. Oncotarget 2013; 4: 1199-1211.

[27] Li W, Cai JH, Zhang J, Tang YX, Wan L. Effects of cyclooxygenase inhibitors in combination with taxol on expression of cyclin D1 and Ki-67 in a xenograft model of ovarian carcinoma. Int J MolSci 2012; 13: 9741-9753.

[28] Rattan R, Graham RP, Maguire JL, Giri S, Shridhar V. Metformin suppresses ovarian cancer growth and metastasis with enhancement of cisplatin cytotoxicity in vivo. Neoplasia 2011; 13: 483-491.

[29] Selvendiran K, Bratasz A, Tong L, Ignarro LJ, Kuppusamy P. NCX-4016, a nitro-derivative of aspirin, inhibits EGFR and STAT3 signaling and modulates Bcl-2 proteins in cisplatin-resistant human ovarian cancer cells and xenografts. Cell Cycle 2008; 7: 81-88.

[30] Liu M, Qi Z, Liu B, Ren Y, Li H, Yang G, Zhang Q. RY-2f, an isoflavone analog, overcomes cisplatin resistance to inhibit ovarian tumorigenesis via targeting the PI3K/AKT/mTOR signaling pathway. Oncotarget 2015; 6: 25281-25294.

[31] Liu X, Gao Y, Shen J, Yang W, Choy E, Mankin H, Hornicek FJ, Duan Z. Cyclin-dependent kinase 11 (CDK11) is required for ovarian cancer cell growth in vitro and in vivo, and its inhibition causes apoptosis and sensitizes cells to paclitaxel. Mol Cancer Ther 2016; 15: 1691-1701.

Supplementary Information

List of antibodies

1. Primary antibodies: Western blotting, FACS, IIF, IHC studies: Rabbit anti-HSP70-2 antibody;

2. Co-localization studies [Calnexin, endoplasmic reticulum marker, sc-70481; GM130, Golgibodies marker, sc-55591; MTCO2, mitochondrial marker, ab3298; Lamin A/C, nuclear envelope marker, sc-7292 and Pan-cadherin, plasma membrane marker, ab6528)];

3. Apoptosis studies [cytochrome-C (sc-13560), Caspase 3 (sc-56052), Caspase 7 (sc-81654), Caspase 9 (sc-56077), PARP1 (CST9532-Full length protein), APAF1 (ab2000), BCL-2 (B3170), Bcl-x$_L$ (B9429), MCL-1 (ab32087), Survivin (ab24479), XIAP (ab2541), cIAP2 (sc-7944), BAX (B8554), BIM (sc-11425), BAK (sc-7873), BAD (sc-8044), BID (sc-11423), PUMA (ab54288) and NOXA (sc-56169)];

4. Cell cycle studies [Cyclin A2 (ab137769), Cyclin B1 (sc-7393), Cyclin D1 (sc-8396), Cyclin E (sc-56310), p16 (sc-9968), p21 (sc-817), p27 (sc-53906), CDK1 (ab18), CDK2 (ab7954), CDK4 (sc-23896), CDK6 (sc-7961), Rb (ab24), p-Rb (ab76298), E2F1 (ab179445)];

5. EMT studies [E-cadherin (ab1416), Cytokeratin 18 (ab668), EMA (ab156947), N-cadherin (ab 76011), SNAIL (ab85931), SLUG (ab51772), VIMENTIN (ab92547), SMA (ab7817), MMP2 (ab92536), MMP3 (ab52915), MMP9 (ab119906), TWIST (ab50887)];

6. Senescence studies: DcR2 (ab2019);

7. Cellular proliferation studies: PCNA (sc-25280);

8. Secondary antibodies: anti-mouse IgG HRP, anti-rabbit IgG HRP, anti-mouse texas red, anti-rabbit IgG FITC (Jacksons ImmunoResearch Laboratories, PA, USA).
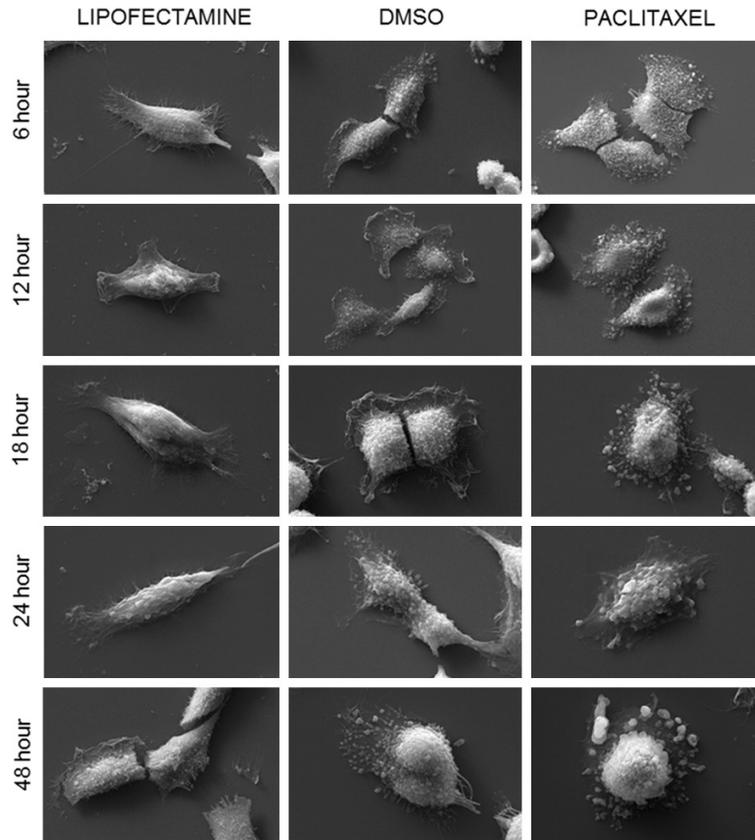
Supplementary Table 1. List of primers of various molecules involved in apoptosis and cell cycle

S. No	Gene	Forward	Reverse
1	*HSP70-2*	CCACAGTGCAGTCGGATATG	GCGATCTCCTTCATCTTCGT
2	*β-actin*	GTTGTCGACGACGAGCG	GCACAGAGCCTCGCCTT
	Apoptosis studies		
1	*Cytochrome-C*	GGCGTGTCCTTGGACTTAGA	TGCCTTTCTCAACATCACCC
2	*Caspase 3*	CTGCCTCTTCCCCCATTCT	TCGCTTCCATGTATGATCTTTG
3	*Caspase 7*	GGTTGAGGATTCAGCAAATGA	GGATCGCATGGTGACATTTT
4	*Caspase 9*	AGGTTCTCAGACCGGAAACA	CTGCATTTCCCCTCAAACTC
5	*PARP1*	TCTGCCTTGCTACCAATTCC	GATGGGTTCTCTGAGCTTCG
6	*APAF1*	TCACTGCAGATTTTCACCAGA	CCTCTCATTTGCTGATGTCG
7	*BCL-2*	CTGAGTACCTGAACCGGCA	GAGAAATCAAACAGAGGCCG
8	*Bcl-x$_L$*	TTCAGTGACCTGACATCCCA	CTGCTGCATTGTTCCCATAG
9	*MCL-1*	TCGTAAGGACAAAACGGGAC	CATTCCTGATGCCACCTTCT
10	*Survivin*	TTGGTGAATTTTTGAAACTGGA	CTTTCTCCGCAGTTTCCTCA
11	*XIAP*	GACCCTCCCCTTGGACC	CTGTTAAAAGTCATCTTCTCTTGAAA
12	*CIAP2*	GTCAAATGTTGAAAAAGTGCCA	GGGAAGAGGAGAGAGAAAGAGC
13	*BAX*	GGGTTGTCGCCCTTTTCTAC	CAGCCCATGATGGTTCTGAT
14	*BIM*	CCTCCCTACAGACAGAGCCA	GATAGTGGTTGAAGGCCTGG
15	*BAK*	CCGAAGCCATTTTTCAGGT	GACCTCCATCTCCACCCTG
16	*BAD*	CAGGCCTCCTGTGGGAC	GGTAGGAGCTGTGGCGACT
17	*BID*	GAGGAGCACAGTGCGGAT	GGAACCGTTGTTGACCTCAC
18	*PUMA*	GACGACCTCAACGCACAGTA	GTAAGGGCAGGAGTCCCAT
19	*NOXA*	AAGTTTCTGCCGGAAGTTCA	GCAAGAACGCTCAACCGAG
	Cell cycle studies		
1	*Cyclin A2*	GGAAGGCATTTTCTGATCCA	GCTAGGGCTGCTAACTGCAA
2	*Cyclin B1*	CAGATGTTTCCATTGGGCTT	GAACCTGAGCCAGAACCTGA
3	*Cyclin D1*	GGCGGATTGGAAATGAACTT	TCCTCTCCAAAATGCCAGAG
4	*Cyclin E*	TCTTTGTCAGGTGTGGGGA	GAAATGGCCAAAATCGACAG
5	*p16*	GTTACGGTCGGAGGCCG	GTGAGAGTGGCGGGGTC
6	*p21*	AGTCAGTTCCTTGTGGAGCC	CATGGGTTCTGACGGACAT
7	*p27*	TTCATCAAGCAGTGATGTATCTGA	AAGAAGCCTGGCCTCAGAAG
8	*CDK1*	GCGGAATAATAAGCCGGGAT	CAACTCCATAGGTACCTTCTCCA
9	*CDK2*	GAATCTCCAGGGAATAGGGC	CTGAAATCCTCCTGGGCTG
10	*CDK4*	TGCAGTCCACATATGCAACA	GTCGGCTTCAGAGTTTCCAC
11	*CDK6*	TGTCTGTTCGTGACACTGTGC	ATGCCGCTCTCCACCAT
12	*Rb*	TCAGTTGGTCCTTCTCGGTC	TGTGAACATCGAATCATGGAA
13	*E2F1*	GGCCAGGTACTGATGGTCA	GACCCTGACCTGCTGCTCT

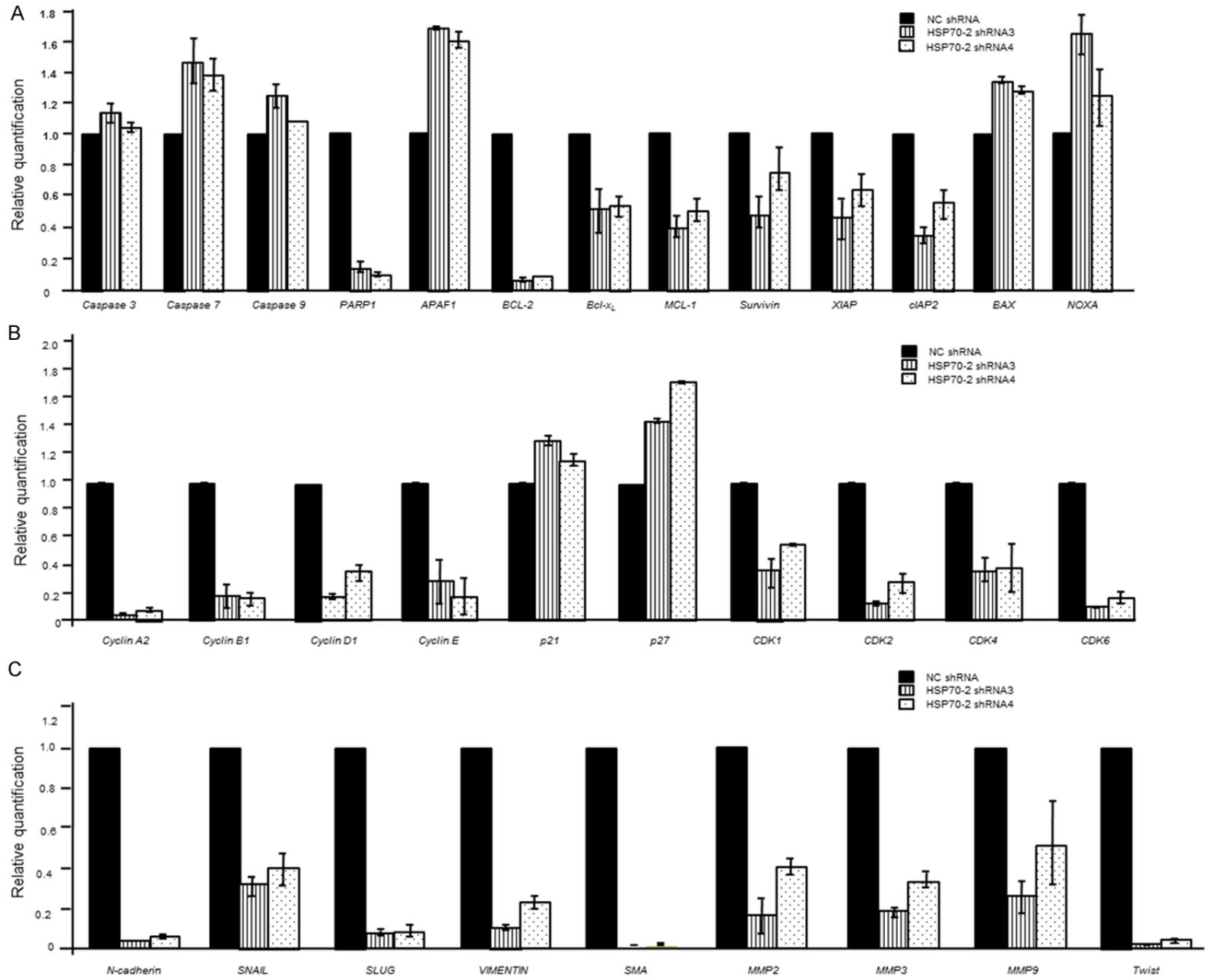**Supplementary Table 2.** List of primers of various molecules involved in EMT studies

	EMT studies		
1	*E-cadherin*	GACCGGTGCAATCTTCAAA	TTGACGCCGAGAGCTACAC
2	*Cytokeratin 18*	GTCAATCTGCAGAACGATGC	GAGCACTTGGAGAAGAAGGG
3	*EMA*	TGGATGGCTCCAGATATTCC	TGTTGATGCTGGCTTTGTTC
4	*N-cadherin*	CCACCTTAAAATCTGCAGGC	GTGCATGAAGGACAGCCTCT
5	*SNAIL*	AGGTTGGAGCGGTCAGC	CCTTCTCTAGGCCCTGGCT
6	*SLUG*	TGACCTGTCTGCAAATGCTC	CAGACCCTGGTTGCTTCAA
7	*VIMENTIN*	ATTCCACTTTGCGTTCAAGG	CTTCAGAGAGAGGAAGCCGA
8	*SMA*	CCAGAGCCATTGTCACACAC	CAGCCAAGCACTGTCAGG
9	*MMP2*	ATGCCGCCTTTAACTGGAG	GGAAAGCCAGGATCCATTTT
10	*MMP3*	AGGGATTAATGGAGATGCCC	CAATTTCATGAGCAGCAACG
11	*MMP9*	ACGACGTCTTCCAGTACCGA	TTGGTCCACCTGGTTCAACT
12	*TWIST*	TCCATTTTCTCCTTCTCTGGAA	GTCCGCGTCCCACTAGC

Supplementary Figure 1. *HSP70-2* gene silencing changes the phenotypic characteristics of ovarian cancer cell, A10. Representative SEM images show no phenotypic changes in cells treated with lipofectamine (negative control). Intense membrane blebbing and apoptotic bodies formation is observed in cells treated with DMSO and Paclitaxel for 6 hours till 48 hours. SEM: Magnification: ×6000, WD = 6 mm, EHT = 20.00 kV.

HSP70-2 promotes ovarian cancer cellular growth and invasion

Supplementary Figure 2. Quantitative-PCR analysis of various genes involved in apoptosis, cell cycle and EMT. A. Histogram depicts the upregulation of *caspase 3, caspase 7, caspase 9, APAF1, BAX, NOXA* while, downregulation of *PARP1, BCL-2, Bcl-x$_L$, MCL-1, Survivin, XIAP and cIAP2* in HSP70-2 shRNA3 and shRNA4 transfected cells compared to NC shRNA transfected ovarian cancer cells. B. Histogram demonstrates fold changes in expression level of genes of cell cycle, *cyclin A2, cyclin B1, cyclin D1, cyclin E, p21, p27, CDK1, CDK2, CDK4* and *CDK6* in NC shRNA, HSP70-2 shRNA3 and shRNA4 transfected ovarian cancer cells. C. Histogram depicts downregulation of mesenchymal markers, *N-cadherin, SNAIL, SLUG, VIMENTIN, SMA, MMP2, MMP3, MMP9* and *TWIST* in HSP70-2 shRNA3 and shRNA4 transfected cells as compared to NC shRNA transfected cells. The three independent experiments were performed in triplicates. Data is represented as mean ± SEM (standard error of the mean).

Supplementary Table 3. Relative quantification of various genes in HSP70-2 depleted A10 ovarian cancer cells

Target gene	NC shRNA	HSP70-2 shRNA3	HSP70-2 shRNA4
Apoptosis studies			
Caspase 3	1	1.14	1.02
Caspase 7	1	1.46	1.39
Caspase 9	1	1.23	1.08
PARP1	1	0.12	0.08
APAF1	1	1.68	1.58
Bcl-2	1	0.05	0.08
Bcl-x$_L$	1	0.48	0.54
MCL1	1	0.41	0.52
Survivin	1	0.50	0.77
XIAP1	1	0.46	0.65
cIAP2	1	0.35	0.58
BAX	1	1.35	1.31
NOXA	1	1.64	1.26
Cell cycle studies			
Cyclin A2	1	0.031	0.079
Cyclin B1	1	0.175	0.151
Cyclin D1	1	0.191	0.352
Cyclin E	1	0.288	0.186
p21	1	1.272	1.153
p27	1	1.436	1.720
CDK1	1	0.373	0.555
CDK2	1	0.131	0.292
CDK4	1	0.369	0.379
CDK6	1	0.088	0.172
EMT studies			
N-cadherin	1	0.030	0.060
SNAIL	1	0.331	0409
SLUG	1	0.068	0.090
VIMENTIN	1	0.098	0.231
SMA	1	0.009	0.0176
MMP2	1	0.167	0.406
MMP3	1	0.187	0.345
MMP9	1	0.267	0.526
TWIST	1	0.019	0.054

Supplementary Table 4. Relative quantification of various genes in HSP70-2 depleted A10 ovarian human xenograft

Target gene	NC shRNA	HSP70-2 shRNA3
Cell cycle studies		
Cyclin A2	1	0.14
p21	1	1.66
p27	1	1.48
CDK1	1	0.69
CDK2	1	0.74
CDK4	1	0.36
CDK6	1	0.38
Rb	1	2.44
E2F1	1	0.46
Apoptosis Studies		
Cytochrome-C	1	3.09
Caspase 3	1	4.38
Caspase 7	1	2.99
Caspase 9	1	1.15
APAF1	1	3.26
Bcl-2	1	0.18
Bcl-x$_L$	1	0.68
MCL-1	1	0.78
XIAP1	1	0.92
BAX	1	1.93
NOXA	1	3.26
EMT studies		
E-Cadherin	1	1.37
Cytokeratin 18	1	2.52
EMA	1	4.63
N-Cadherin	1	0.10
SNAIL	1	0.30
SLUG	1	0.66
VIMENTIN	1	0.83
SMA	1	0.24
MMP2	1	0.37
MMP3	1	0.17
MMP9	1	0.75
TWIST	1	0.85
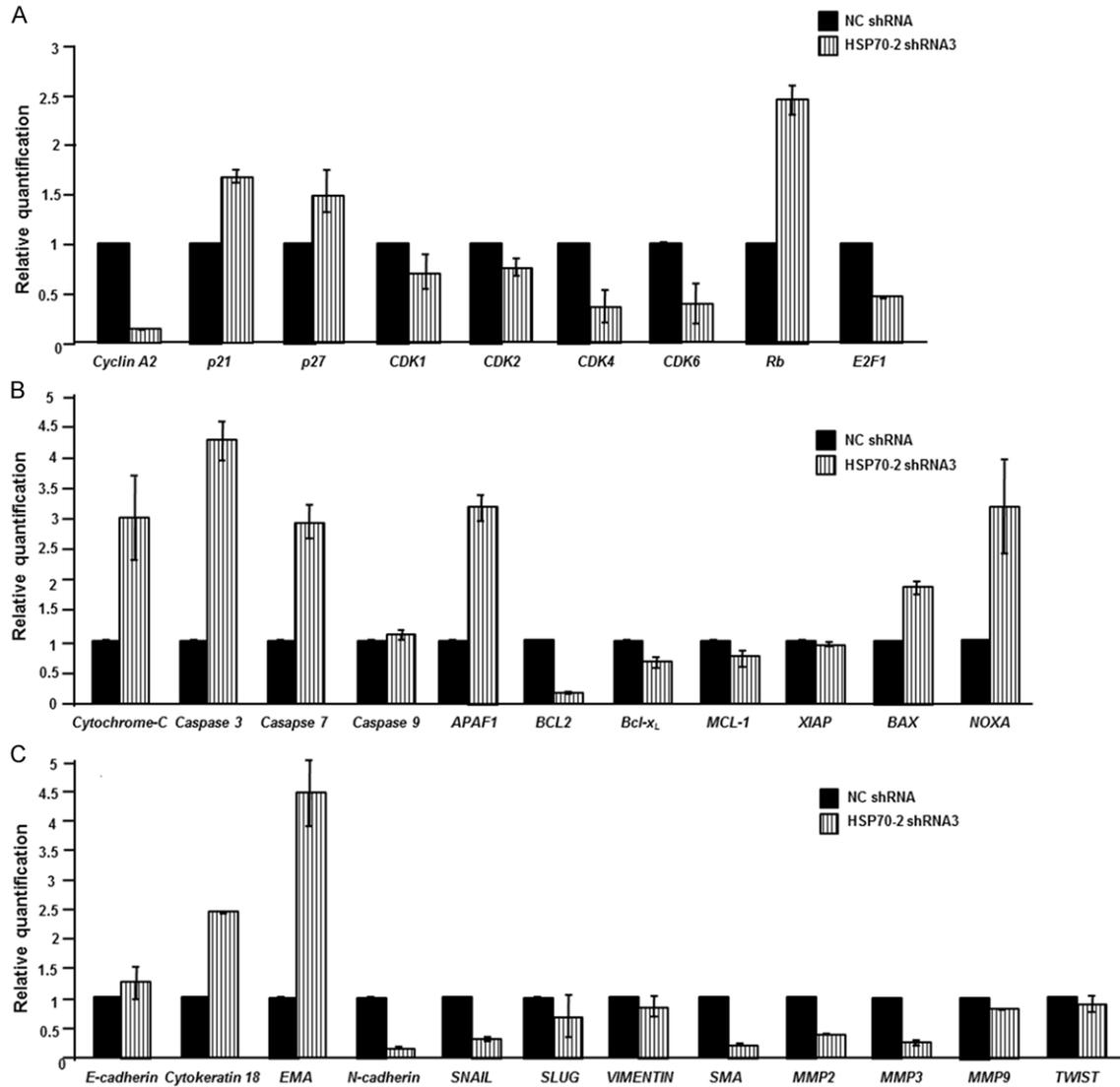
Supplementary Figure 3. Quantitative-PCR analysis of various genes involved in cell cycle, apoptosis and EMT in xenograft tumor cells. A. Histogram demonstrates difference in expression level of genes of cell cycle, *cyclin A2, p21, p27, CDK1, CDK2, CDK4, CDK6, Rb* and *E2F1* in NC shRNA and HSP70-2 shRNA3 treated tumor. B. Histogram depicts upregulation of *cytochrome-C, caspase 3, caspase 7, caspase 9, APAF1, BAX and NOXA*; and downregulation of *PARP1, BCL-2, Bcl-x$_L$, MCL-1* and *XIAP* in HSP70-2 shRNA3 treated tumor as compared to NC shRNA treated tumor. C. Histogram depicts upregulation of epithelial markers like *E-cadherin, cytokeratin 18* and *EMA* and downregulation of mesenchymal markers, *N-cadherin, SNAIL, SLUG, VIMENTIN, SMA, MMP2, MMP3, MMP9* and *TWIST* in HSP70-2 shRNA3 as compared to NC shRNA treated tumor. The three independent experiments were performed in triplicates. Data is represented as mean ± SEM (standard error of the mean).